

Ammonia/hydrogen mixtures in an SI-engine: Engine performance and analysis of a proposed fuel system

C.S. Mørch^{*}, A. Bjerre, M.P. Gøttrup, S.C. Sorenson, J. Schramm

Department of Mechanical Engineering, Technical University of Denmark, Nils Koppels Allé Building 403, DK-2800 Kgs. Lyngby, Denmark

ARTICLE INFO

Article history:

Received 16 April 2009

Received in revised form 17 September 2010

Accepted 21 September 2010

Keywords:

Ammonia

Hydrogen

Engine

ABSTRACT

In recent years there has been increasing focus on using metal ammine complexes for ammonia storage. In this paper a fuel system for ammonia fuelled internal combustion engines using metal ammine complexes as ammonia storage is analyzed. The use of ammonia/hydrogen mixtures as an SI-engine fuel is investigated in the same context. Ammonia and hydrogen were introduced into the intake manifold of a CFR-engine. Series of experiments with varying excess air ratio and different ammonia to hydrogen ratios was conducted. This showed that a fuel mixture with 10 vol.% hydrogen performs best with respect to efficiency and power. A comparison with gasoline was made, which showed efficiencies and power increased due to the possibility of a higher compression ratio. The system analysis showed that it is possible to cover a major part of the necessary heat using the exhaust heat. It is proposed to reduce the high NO_x emissions using SCR as exhaust after treatment.

© 2010 Elsevier Ltd. All rights reserved.

1. Introduction

In the presented work mixtures of ammonia and hydrogen are investigated as SI-engine fuels. The idea was to use a metal amine complex to store ammonia. By using the exhaust heat, the ammonia could be desorbed at the rate used. Then the ammonia could be partially decomposed into hydrogen and nitrogen in order to obtain the best hydrogen to ammonia ratio. This paper addresses the performance of such fuel in a Cooperative Fuel Research-engine (CFR) SI-engine. A possible configuration of a fuel system using the metal amine complex Mg(NH₃)₆Cl₂ as ammonia carrier is presented in [Appendix 1](#).

1.1. Ammonia and hydrogen mixtures as SI-engine fuel

Through the years a lot of investigations on hydrogen as an engine fuel have been made. Many of these investigations have shown hydrogen as a suitable fuel for the spark ignited internal combustion engine. However, problems with abnormal combustion such as backfire have been widely reported. An overview of these experiences has been made by Verhelst et al. [1]. With ammonia the number of investigations is limited [2–6]. They show that it is possible to use ammonia as a fuel for SI-engines. With the decomposition of a small amount of ammonia equaling a hydrogen content of approximately 1% by mass (approximately 8 vol.%), the

performance was satisfactory. An advantage of ammonia and hydrogen is that they do not contain carbon, eliminating emissions of carbon oxides from the engine. Reiter and Kong [7] found that in a compression ignition engine using ammonia in combination with diesel the emissions of NO_x was not higher compared to running on diesel fuel alone.

In [Table 1](#) some fuel properties of ammonia, hydrogen and gasoline are given. The octane rating of both ammonia and hydrogen is higher than gasoline, making it preferable to run at a higher compression ratio (CR). The flame velocity and the min. ignition energy of ammonia and hydrogen are far apart. By mixing it was hoped that a suitable compromise could be gained. The ammonia to hydrogen ratio presents a new possible engine control parameter.

2. Experimental methods

In order to investigate the ammonia hydrogen mixtures as SI-engine fuel preliminary experiments with varying fuel mixtures were made, the results were to be evaluated with respect to performance and efficiency.

The fuel system was designed to resemble the proposed fuel system presented in [Appendix 1](#). Since the ammonia is released from the metal ammine complex as a gas the fuel was introduced to the manifold in the gaseous state. In order to simplify the setup, pressurized hydrogen and ammonia were used as fuel. The external mixture formation will reduce the air flow to the engine due to the charge dilution by the gaseous fuel in the intake charge. Because of this it was expected that the indicated mean effective pressure would be lower compared to a solution where the fuel

^{*} Corresponding author. Tel.: +45 29721680.

E-mail addresses: pub@csmoerch.dk (C.S. Mørch), scs@mek.dtu.dk (S.C. Sorenson), js@mek.dtu.dk (J. Schramm).

Table 1

Some fuel properties of ammonia, hydrogen and gasoline. Data from [8–10].

		Ammonia	Hydrogen	Gasoline
Lower heating value	MJ/kg	18.8	120.0	44.5
Flammability limits, gas in air	vol.%	15–28	4.7–75	0.6–8
Laminar flame velocity	m/s	0.015	3.51	0.58
Autoignition temperature	°C	651	571	230
Absolute min. ignition energy	mJ	8.0	0.018	0.14
Octane rating, RON	–	>130	>100	90–98
Density, 25 °C, 1 atm	g/L	0.703	0.082	740

is injected directly in the cylinder. At stoichiometric conditions the intake air flow is reduced by 22.5–30% depending on the content of hydrogen in the mixture.

2.1. Description of the experimental setup

For the experiments a CFR-engine in SI-setup with a shrouded intake valve was used. The engine has a bore of 82.6 mm and a stroke of 114.3 mm with a displacement of 612.5 cm³. The intake valve opens and closes at 10 CAD ATDC (Crank Angle Degree After Top Dead Centre) and at 34 CAD ABDC (After Bottom Dead Centre) respectively. The exhaust valve opens at 40 CAD BBDC (Before Bottom Dead Centre) and closes at 15 CAD ATDC.

The fuel flow was controlled with two M + W Instruments mass flow controllers (D-5121 and D-6270). A National Instruments data acquisition board and LabVIEW were used to set the desired flow and also handled different data logging during the experiments. A diagram with the main components of the fuel system is shown in Fig. 1.

The standard intake manifold and carburetor were replaced with a custom intake manifold. The air pipe of the manifold had an inner diameter of 28.5 mm, while the fuel pipes had an inner diameter of 17.3 mm. The fuel pipes were welded on the air pipe, approximately 180 mm from the engine mounting, opposed to each other at an angle of 45 degree with the air pipe.

The exhaust manifold was not altered for the experiments, but was equipped with a k-type thermocouple mounted directly downstream of the cylinder head. The exhaust was also equipped with a portable Horiba 240-CL gas analyzer. This analyzer contains

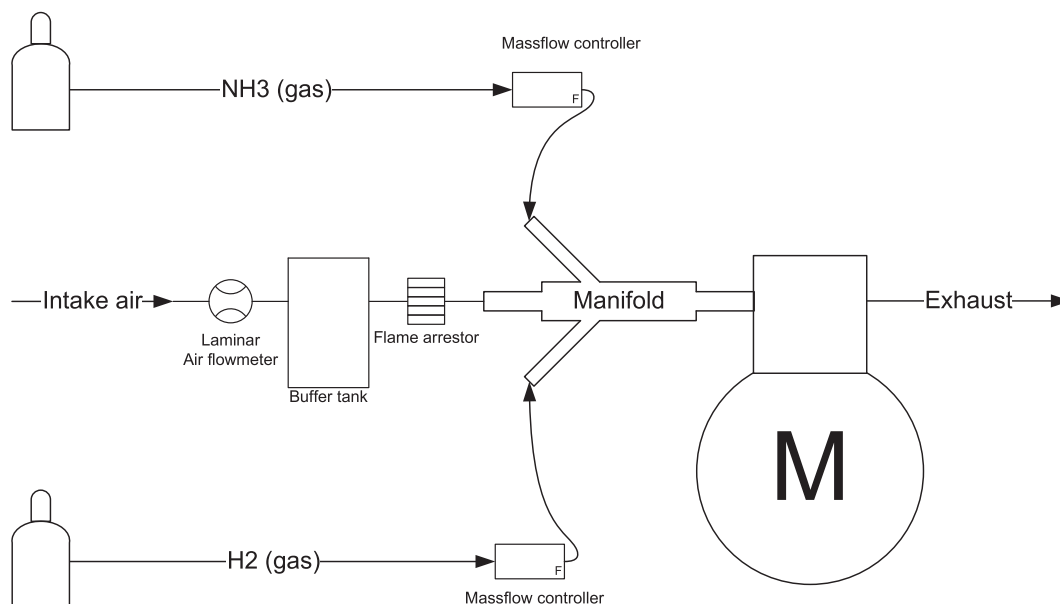
an electro-chemical O₂ detector that was used to check the excess air ratio. The excess air ratio was calculated on laminar flow measurements of the intake air together with the fuel flow. The analyzer also has a chemiluminescence NO_x detector.

The cylinder pressure was measured with a Kistler water cooled piezo-electric pressure pickup installed in the cylinder head. The signal was amplified with a Kistler KIAG 5001 charge amplifier. The pressure measurements were timed with a shaft encoder giving 720 pulses per revolution, which gives a cylinder pressure resolution of 0.5 CAD.

Ammonia and hydrogen have a higher octane rating than gasoline making a higher CR attractive. To raise the CR above 10:1 a modification of the piston was made. The piston height was increased by adding a 4.9 mm thick steel disk to the top of the piston. In order to ensure good ignition conditions a groove was milled in the steel disc in front of the side mounted spark plug.

2.2. Heat release analysis

The sampled cylinder pressure data were used to conduct a heat release analysis. The analysis was made with an adaptation by Mørch [11] of the two zone model proposed by Krieger and Borman [12]. The model assumes that at any instant during combustion, the chamber volume can be divided into a burned and unburned volume separated by an infinitesimally thin flame front. The cylinder pressure is assumed uniform and each volume is assumed to have a uniform temperature. The thermodynamic properties of the unburned gas are calculated on the basis of a frozen composition determined by the stoichiometry of the actual charge. Krieger and Borman proposed that the composition of the burned gas was determined with full chemical equilibrium [12]. However, in this work the ideal composition of the complete combustion products has been used. The geometric shape of the two volumes was assumed to be cylindrical, with the burnt volume cylinder inside the unburned. It is assumed that no heat transfer occurs between the two volumes, and as such the only surfaces of the burned volume that are subject to heat transfer are the cylinder top and piston. Furthermore, it is assumed that the surfaces of the combustion chamber are uniform in temperature. The mean temperature for all the surfaces was set to 150 °C. In the current calculations the heat transfer coefficient was found

**Fig. 1.** Diagram showing the fuel system setup for the experiments.

by the Eichelberg correlation [13]. The heat release model does not take blow-by or flow into crevices into account. For a more in depth description of the mathematical model and the numerical solution see [11].

2.3. The experiments conducted

Ammonia/hydrogen mixtures were tested containing 5–100 vol.% hydrogen and the CR was varied from 6.23 to 13.58. The excess air ratio was varied from the leanest possible to a mixture that was on the rich side of stoichiometric. The leanest possible mixture varies with the fuel mixture, but corresponds to a brake mean effective pressure of 250–300 kPa. It was possible to operate the engine on pure ammonia but with a strong tendency to cut out. The addition of 5 vol.% hydrogen made the engine run smoothly. All tests were made with a MBT spark timing.

3. Engine performance results

In Fig. 2a–d the results from the first set of experiments are shown. In general it is seen that the best efficiency is found at an excess air ratio slightly higher than 1 and that the highest mean effective pressure is found at an excess air ratio slightly lower than 1. It is also seen that an increase in CR gives a better indicated efficiency and mean effective pressure. These tendencies are common with SI-engines.

The most interesting observation is that in general the lowest indicated efficiency and mean effective pressure are found for mixtures containing much hydrogen. This is presumably caused by the higher intake air dilution of hydrogen compared to ammonia.

In the second set of experiments the piston was modified as described and the main focus was moved to investigating higher CR and excess air ratios close to stoichiometric. These results are presented in Fig. 2e and f. In Fig. 2f the indicated mean efficiency is almost the same for CR 11.64 and 13.58 and about 2 % points higher than the results presented in Fig. 2c. The indicated mean effective pressure increased to a maximum of 725 kPa at CR 13.58 and 10 vol.% H_2 .

In Fig. 2e and f there is also plotted a reference series run on 95 RON octane gasoline at a CR of 7.12 on the same engine. The CR of 7.12 represents the knock limited CR for the CFR-engine when running on gasoline. When seen in comparison the ammonia/hydrogen mixtures and the gasoline results have a almost similar indicated mean effective pressure. The higher CR compensates for the reduced air flow caused by the intake air dilution. This is very relevant in relation to practical implementation of ammonia/hydrogen mixtures as SI-engine fuel. By raising the CR it is possible to achieve a similar power output without using a larger engine. Besides a similar power output, ammonia and hydrogen mixtures at high CR yield a significantly higher indicated efficiency than the gasoline reference at the lower CR. This can be seen in Fig. 2e.

3.1. Heat release

In Fig. 3 a number of graphs from the heat release analysis are shown. All calculations are made from the time of ignition until the exhaust valve opens. Because it was not possible to estimate the heat loss from any of the measurements, the Eichelberg correlation was not scaled or modified in any way.

The top curves show the influence of the fuel mixture hydrogen content on the mass burn rate. There are quite a few oscillations with 100 vol.% hydrogen compared to the 10 vol.% hydrogen, which are due to the pressure oscillation originating from the very fast flame propagation (pressure data can be seen in Fig. 4). The

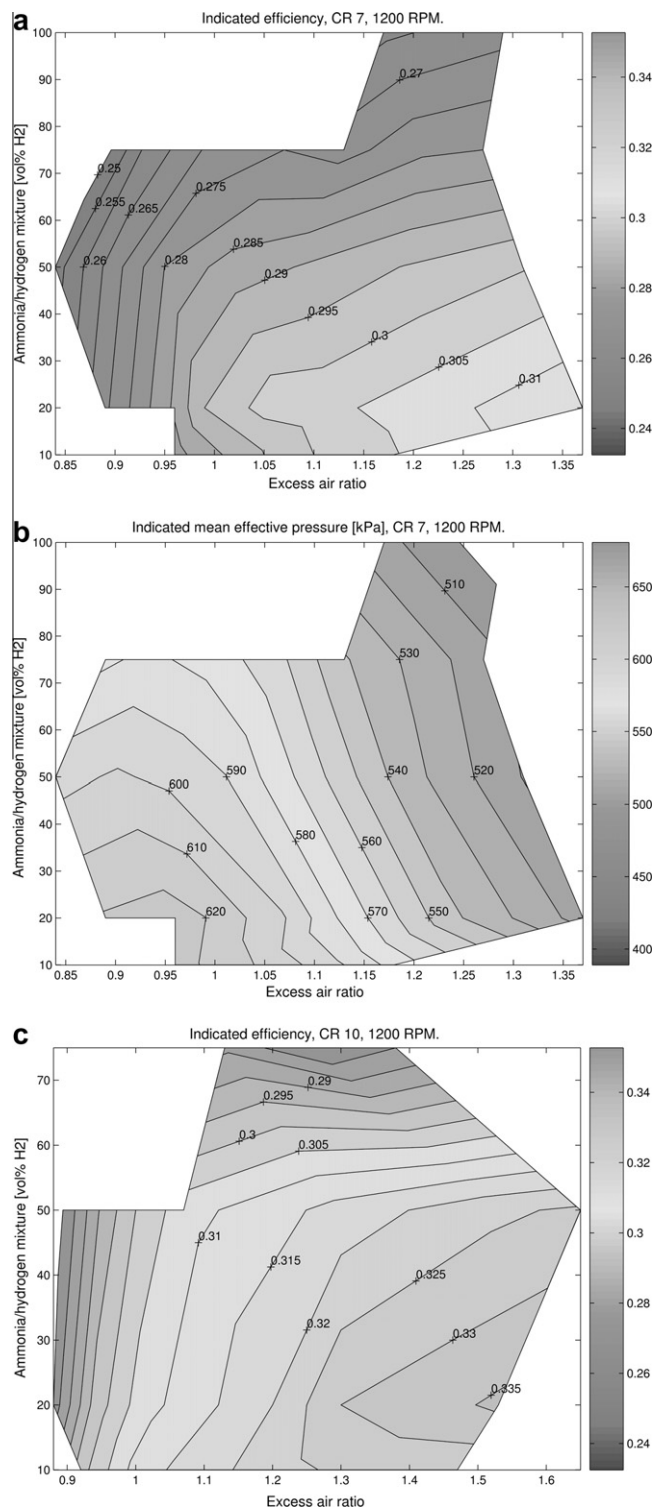


Fig. 2. Performance plots. Plots showing the indicated efficiency and the indicated mean effective pressure versus the excess air ratio and the ammonia/hydrogen mixture for figures (a–d). (a) η_i , CR 6.23, 1200 rpm (b) imep [kPa], CR 6.23, 1200 rpm (c) η_i , CR 8.9, 1200 rpm (d) imep [kPa], CR 8.9, 1200 rpm (e) η_i , varying CR, 1200 rpm (f) imep [kPa], varying CR, 1200 rpm.

fast combustion of hydrogen is also illustrated by the peak mass burn rate that is more than double the mass burn rate of the 10 vol.% H_2 mixture. The pressure oscillations give a significantly higher heat loss than described by the Eichelberg equation. Shudo and Suzuki conclude in a comparison between different known heat transfer correlations [14], that none of them represent the

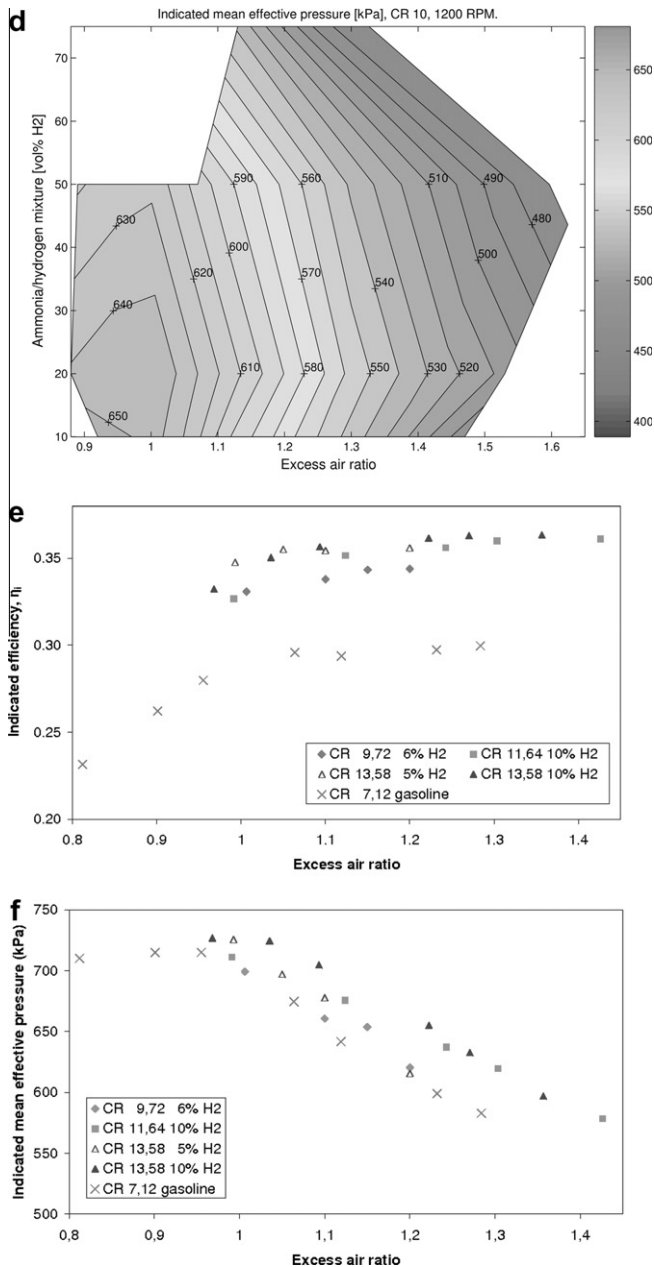


Fig. 2 (continued)

heat transfer experienced during hydrogen combustion in a satisfactory way. As a consequence they propose that a new heat transfer correlation appropriate for hydrogen combustion should be developed, which incorporates the effect of the faster gas dynamics due to the fast flame propagation of hydrogen. The falling tendency of the mass fraction burned curve of the 100 vol.% H₂ mixture from 15 degrees after ignition, indicates that the heat loss is actually a lot higher at the end of the combustion.

As mentioned earlier the piston was modified in order to raise the CR of the CFR-engine. This modification had an effect on the heat release. After the modification the start of the combustion was faster and the end of the combustion faded out slower at comparable CR. This is illustrated in the centre graph in Fig. 3. The pressure data for the heat release curve at CR 8.9 were taken before the modification and the corresponding data for the CR 9.6 curve were taken after the modification. Although the CR is not the same, there are some clear tendencies that differ, which can be seen. After the modification the mass burn rate curve seems to have two peaks.

This becomes more evident when the burn rate for the CR 13.56 is analyzed. It was noted that the peak cylinder pressure was a little lower after the modification as well. These tendencies are the same as described by Taylor, indicating increased turbulence in the combustion chamber [15]. For this reason the measurements before and after the modification cannot be compared directly. In spite of the modifications, the results in Fig. 2 show that the imep and the efficiency increase with the CR.

According to Heywood it is expected that the gross mass fraction burned reaches a value of 0.93–0.98 [16]. The fact that the flow into crevices and piston blowby are not incorporated in the heat release calculations may be some of the explanation to why the mass fraction burned only reaches 0.85–0.9, in the bottom graph in Fig. 3. Another explanation is that the applied correlation for the heat transfer is not scaled to the actual case or that it is insufficient in describing the heat loss from ammonia/hydrogen mixtures.

4. Results of the system analysis

The exhaust temperatures used in the calculation and the fuel and airflows were determined from the experiments on the CFR engine fuelled with ammonia/hydrogen mixtures. A desorber pressure of 3 bars was assumed, which corresponds to the actual fuel pressure used in the experiments.

As expected, the fraction covered by the exhaust (f_{cbe}) depends strongly on the exhaust temperature, which is shown in Fig. 5. Because the decomposition of ammonia requires additional heat, it was expected that mixtures containing high amounts of hydrogen would have a lower heat fraction covered by the exhaust. In Fig. 6, the maximum heat fraction in each series of experiments is shown. In each of the series the maximum value of f_{cbe} corresponds to the maximum exhaust temperature, which in all the cases was attained at a near stoichiometric fuel/air ratio. In Fig. 5 it is also seen that the hydrogen content of the mixture does not have dramatic impact on f_{cbe} . It seems that the additional heat needed for the mixtures with high hydrogen content is to some extent counterbalanced by the higher exhaust temperatures. The lower exhaust temperature of the mixtures with highest hydrogen content in Fig. 6, is caused by an excess air ratio higher than stoichiometric. It was not possible to run the CFR-engine at stoichiometric conditions with high hydrogen content.

The evaluation clearly shows that if the proposed fuel system is used, it is not possible to cover the required heat only using the exhaust heat. An alternative approach must be taken. A possible solution is to retard the ignition timing in order to raise the exhaust temperature. Of course the rise in temperature comes at the cost of a lower efficiency and power output. In Fig. 7 the fraction of heat covered, the brake thermal efficiency and the exhaust temperature are plotted as a function of the ignition timing.

As expected, the heat fraction covered by the exhaust rises concurrently with the exhaust temperature as the ignition timing is retarded. Even when the timing is set to 5 °C before top dead center the heat fraction covered barely reaches 50%, while at the same time the brake thermal efficiency is reduced from approximately 20% to 15%. Furthermore the engine is unstable at this late ignition so retarding the timing is not a feasible solution.

In the proposed fuel system, the desorber pressure is 3 bar(a). If it is lowered to 0.5 bar(a) the equilibrium temperature of reaction (A1a), which is the limiting reaction, is lowered to 350 °C. The consequence of the lower temperature with a compression ratio of 10:1, an engine speed of 1200 rpm and a fuel mixture with 10 vol.% hydrogen is that the maximum heat fraction covered is raised from 27% to 43%. It is clear that such a lowering of the pressure in the desorber is not sufficient if the goal is a 100% coverage

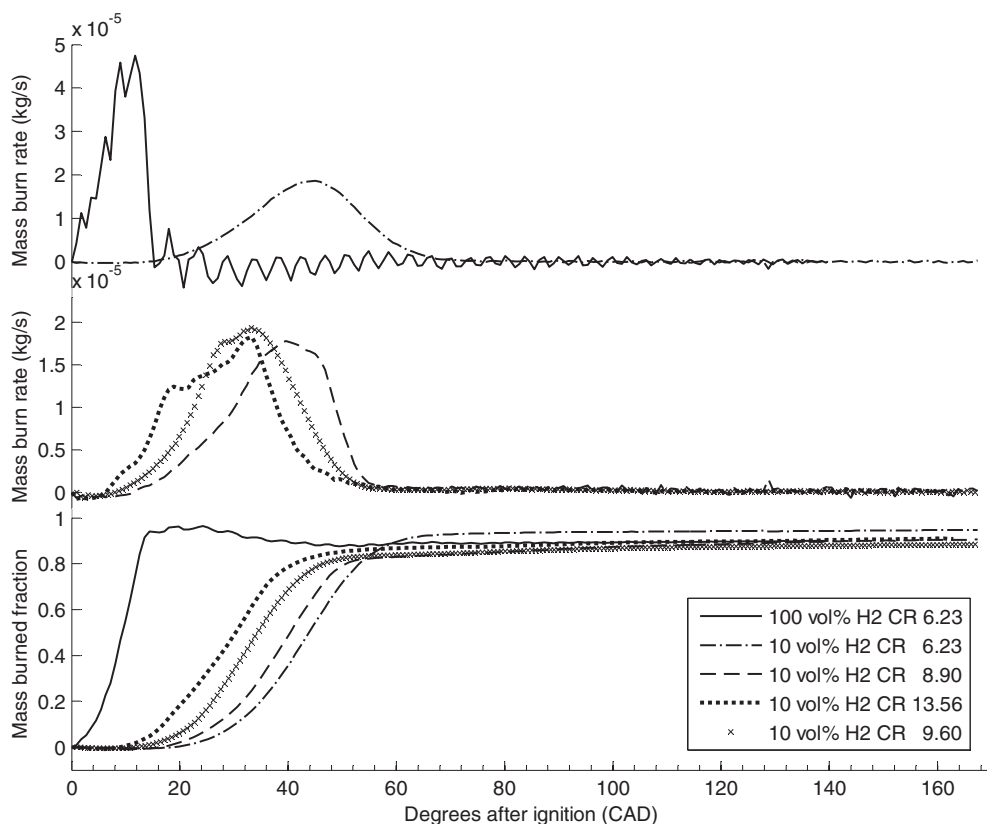


Fig. 3. Heat release curves. Top curves: The mass burn rate for combustion at CR 6.23 for mixtures containing 100 and 10 vol.%, respectively. Center curves: The mass burn rate for three different CR before (CR 6.23 and 8.90) and after (CR 9.60 and 13.56) the piston modification. Bottom curves: Mass burned fraction for all five curves. All the curves are based on the mean pressure trace of 50 consecutive cycles.

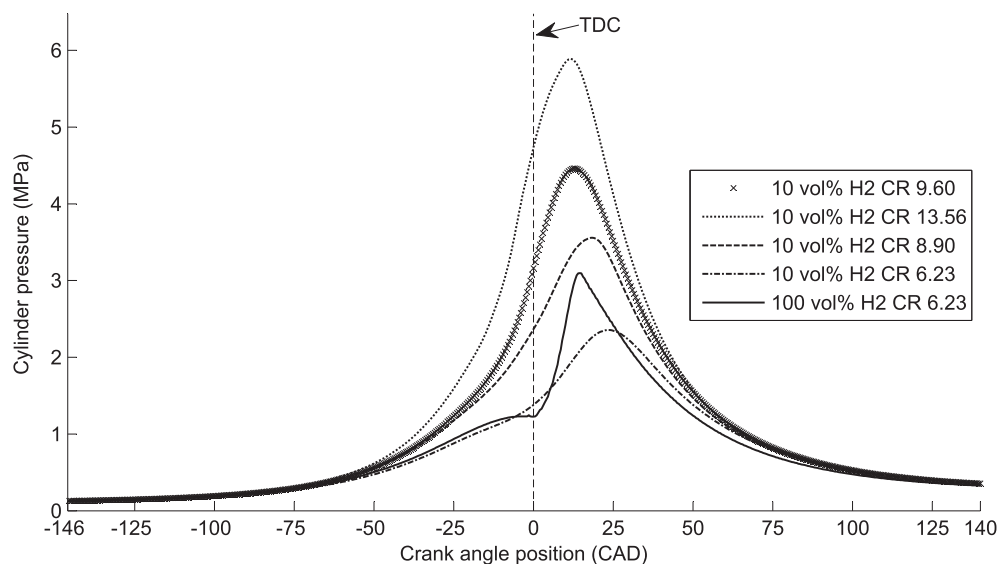


Fig. 4. Pressure traces. Mean pressure traces for the five heat release curves shown in Fig. 3.

of the necessary fuel system heat from the exhaust. Furthermore it must be taken into account that some kind of pressure rise after the desorber is necessary in order to introduce the fuel into the intake manifold where the pressure is in the order of 1 bar(a). Such a pressure rise would of course also cost additional energy.

Another approach to the problem would be to accept that not all the ammonia in the metal ammine complex can be desorbed. If it was accepted that only 2/3 of the stored ammonia was des-

orbed, then the only reaction to be taken into account is reaction (A1c), which means that the equilibrium temperature and the reaction enthalpy is lowered. If only 2/3 of the ammonia is desorbed, the energy density is lowered, which has an effect on the overall vehicle efficiency since more weight and volume have to be carried if the same range is required. If the metal ammine complex is re-loaded as proposed by Elmøe et al. [17], the ammonia that cannot be desorbed is not wasted as it is recycled in the reloading process.

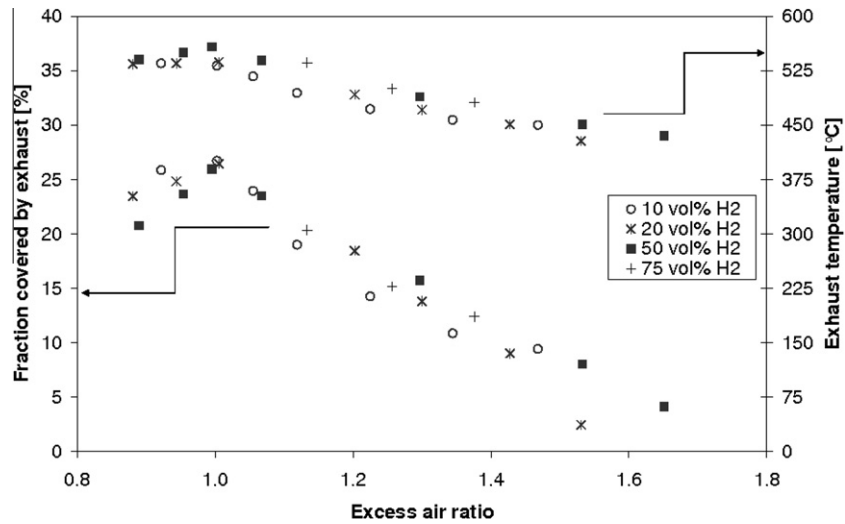


Fig. 5. Heat covered by exhaust. The fraction of the needed heat for the fuel system covered by the exhaust heat (f_{cbe}) and the exhaust temperature (T_{exh}) as a function of excess air ratio. The compression ratio is 8.9:1 and the engine speed 1200 rpm.

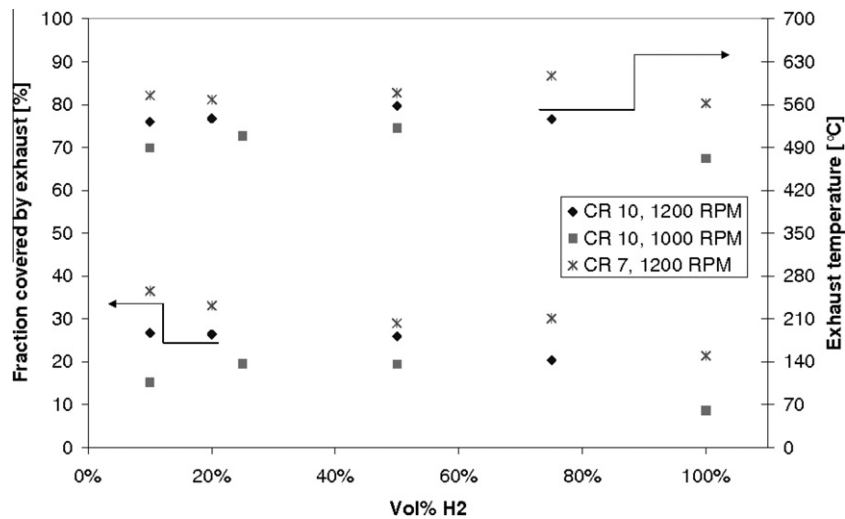


Fig. 6. Maximum heat covered by exhaust. The maximum fraction of the needed heat for the fuel system covered by the exhaust heat in each series of experiments. The corresponding maximum exhaust temperature is also shown.

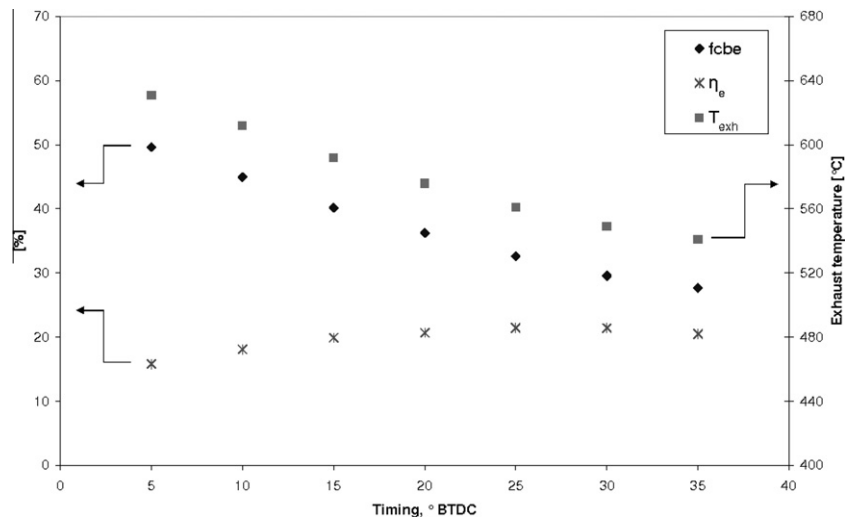


Fig. 7. The variation of the fraction covered by exhaust (f_{cbe}), the brake thermal efficiency (η_e) and the exhaust temperature (T_{exh}) with ignition timing. The compression ratio is 6.23:1, the engine speed 1200 rpm and a stoichiometric fuel mixture with 20 vol.% H_2 was used.

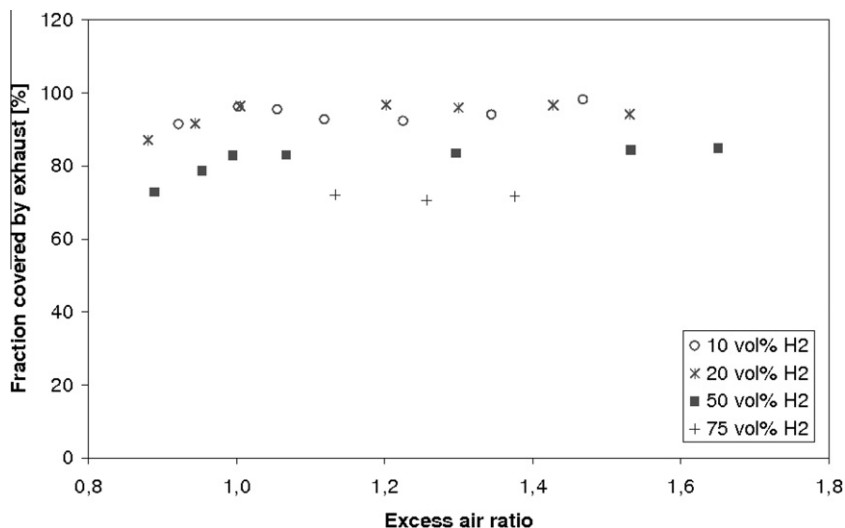


Fig. 8. Heat covered by exhaust with 2/3 of ammonia desorbed. The fraction of the needed heat for the fuel system covered by the exhaust heat (f_{cbe}) as a function of excess air ratio. The compression ratio is 8.9:1 and the engine speed 1200 rpm. 2/3 of the ammonia is desorbed from the metal ammine complex. The desorber temperature is 150 °C which corresponds to a pressure of 2 bar(a).

At a desorber pressure of 3 bar, the acceptance of less desorbed ammonia lowers the equilibrium temperature to 169 °C. This means that the maximum heat fraction covered, in the same example as before, is raised to 96 %. If the desorber pressure is lowered from 3 to 2 bar(a), which is well above the manifold pressure, the equilibrium temperature is reduced to 150 °C. The new heat fraction covered, with the same data as in Fig. 5, is shown in Fig. 8. It is seen that the heat fraction covered is now closer to a 100 %. In the case of 10 vol.% hydrogen some cases are even above 100%. The fuel mixtures with 50 and 75 vol.% have a lower fraction covered, the reason for this is that energy needed for the decomposition of ammonia is more significant when the energy need for the desorption is lowered. However, it must be stressed that in the evaluation made here, transient operation including startup is not taken into account. A fuel system without loss, as assumed here, is of course also not possible in real life. As a result of this,

it is not likely that all the needed heat for the fuel system can be covered by the exhaust heat, but the analysis shows that if care is taken in the design of the system, it is possible to cover a major part of the required heat with the exhaust. It must also be taken into account that in an engine that runs at a higher speed than the CFR-engine used here, a higher exhaust temperature can be expected, because of lower relative heat loss to the cylinder walls. Our own measurements on production engines show a 150–200 °C higher exhaust temperature at higher engine speeds (>2000 rpm).

If additional heat for the fuel system is needed, the most efficient way to achieve this is to use some of the fuel directly to raise the exhaust temperature. The alternative is to use some kind of electrical heating.

It would probably be necessary to use electrical heating during start-up, however it is advisable to restrict the use to such situations.

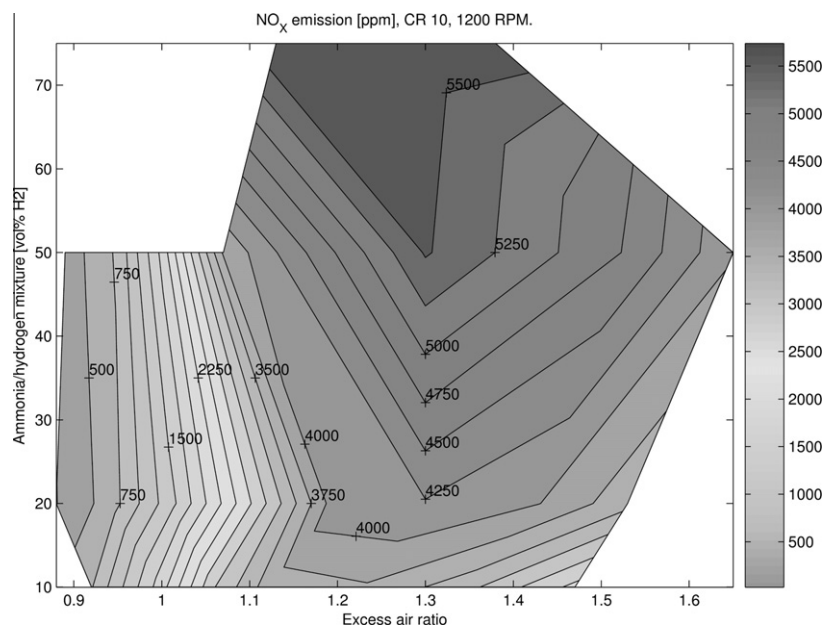
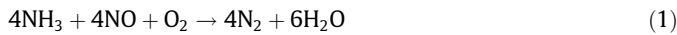


Fig. 9. NO_x emissions. Plot showing experimental NO_x emissions at CR 8.9 and 1200 rpm.

5. Reduction of nitric oxide emissions

With most SI-engines NO_x formation has to be taken into account. In Fig. 9, experimentally determined NO_x emissions from the CFR-engine running on ammonia/hydrogen mixtures are shown. The NO_x emissions are plotted as a function of the hydrogen content of the fuel mixture and the excess air ratio. The figure clearly shows that the largest NO_x emissions occur with a high hydrogen content and an excess air ratio between 1.1 and 1.4. The reason for this is the high amount of thermal NO_x that is created due to the high combustion temperature of hydrogen. During the experimental investigation it was found that the engine had the best power output at an excess air ratio of 1 and 10 vol.% hydrogen content. At this operating point there is still a substantial NO_x emission. It has not been possible to determine the amount of fuel NO_x which is expected to be substantial, due to the molecular content of nitrogen in the fuel. Variation of ignition timing with 20 vol.% hydrogen did not show a significant variation of the measured NO_x emissions. This tendency indicates that fuel NO_x dominates over the thermal NO_x mechanism, which is substantially influenced by the variation of ignition timing. With gasoline fuelled SI-engines a variation of the ignition timing is expected to strongly influence the NO_x emission [16]. On a similar CFR engine fuelled with gasoline Huls et al. [18] reported NO_x emissions in the range of 1000–5500 ppm depending on the mixture strength. Compared to the emissions measured here it must be concluded that in spite of the differences between the NO_x formation mechanisms of gasoline and hydrogen/ammonia fuel, the total emission levels of NO_x are very similar. This result is in agreement with the results of Reiter and Kong [7].

Using ammonia as an engine fuel makes the use of SCR (Selective Catalytic Reduction) of these nitric oxides attractive since ammonia is already on board the vehicle. Using SCR to reduce the NO_x emissions would not require significant amounts of ammonia since the overall reaction has a consumption ratio of 1:1 (molar base) as shown by:



The temperature interval of the reaction is 600–700 K [19], which fits well to the exhaust gas temperature. Since the SCR reaction is exothermic it would not have a negative effect on the ammonia desorption process.

The main challenge of using SCR on board a vehicle is to avoid major ammonia slip at varying load conditions.

6. Conclusion and suggestions

An experimental setup for testing ammonia/hydrogen mixtures in an SI-engine has been developed and some basic experiments were made. This investigation gave some preliminary results and trends that could be used in further work.

- Ammonia/hydrogen mixtures constitute a very suitable fuel for SI engines.
- The efficiency and mean effective pressure were highest at mixtures containing 10 vol.% hydrogen in the fuel, presumably because of the higher heat loss during combustion of the mixtures with high levels of hydrogen.
- Due to the higher octane rating of ammonia/hydrogen mixtures it is possible to compensate for the intake air dilution by increasing the compression ratio.

A further investigation of the engine performance in a broader operating area, is necessary to draw a final conclusion. The heat release and, especially the heat loss from mixtures, with high hydro-

gen levels should be investigated further. It is of high importance investigate the mixtures performance at higher engine speeds.

In order to investigate the possibility of using MgCl_2 as an ammonia carrier for the use as SI-engine fuel, a fuel system was simulated. The model was used to analyze the possibility of using exhaust heat for the desorption and decomposition of ammonia.

The investigation shows that it is possible to cover a major part of the needed heat for a metal ammine complex based fuel system with exhaust heat.

The largest NO_x emissions occur with a high hydrogen content and an excess air ratio between 1.1 and 1.4. For reduction of NO_x it is proposed to use SCR since ammonia is already onboard. The overall emission levels of NO_x on ammonia/hydrogen and gasoline are the same.

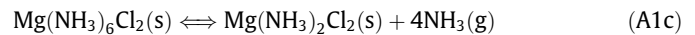
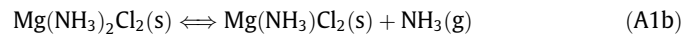
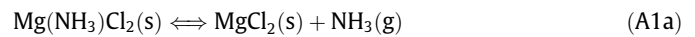
Appendix 1. The metal ammine complex storage system

A1.1. Introduction

The concept of using metal ammine complexes for hydrogen storage was introduced in 2005 by Christensen et al. [20]. The hydrogen is stored as ammonia absorbed in the complex. When the hydrogen is needed, the ammonia is desorbed from the metal ammine complex and is then decomposed to hydrogen and nitrogen. At the time the concept was introduced, it was suggested that the hydrogen and possibly the ammonia could be used in fuel cells. As such, the metal ammine complex offers a solution to the problem of storing hydrogen for use in transportation. In this work a possible fuel system for an SI engine for use in a vehicle is presented which uses $\text{Mg}(\text{NH}_3)_6\text{Cl}_2$ as an ammonia carrier and utilises the exhaust heat to desorb the ammonia.

According to Christensen et al. metal ammine complexes, e.g. $\text{Mg}(\text{NH}_3)_6\text{Cl}_2$, offer a fully reversible storage method for ammonia and subsequently also hydrogen [20]. The method consists in principle of the four stages shown in Fig. A1. The first two stages are assumed to be carried out in centralized plants or at the filling station. The last two stages have to be carried out onboard the vehicle.

The desorption and absorption of ammonia are characterized by the following three reactions [21]:



The factors that determine whether the ammonia is absorbed or desorbed are the bulk temperature and pressure. This yields the following relationship ([2 Eqs. (5) and (6)]):

$$p_{\text{des}} - p_{\text{eq}} \begin{cases} < 0 \text{ desorption} \\ = 0 \text{ equilibrium} \\ > 0 \text{ absorption} \end{cases} \quad (\text{A2})$$

$$T_{\text{des}} - T_{\text{eq}} \begin{cases} < 0 \text{ absorption} \\ = 0 \text{ equilibrium} \\ > 0 \text{ desorption} \end{cases} \quad (\text{A3})$$

where T_{des} and p_{des} are the bulk temperature and pressure of the ammonia desorber. The relation between the equilibrium temperature (T_{eq}) and pressure (p_{eq}), is given by [2 Eq. (4)]:

$$T_{\text{eq}} = \frac{-\Delta H_{r,k}}{\ln p_{\text{eq}} \cdot R - \Delta S_{r,k}} \quad (\text{A4})$$

$\Delta H_{r,k}$ denotes the reaction enthalpy of the k th reaction, R is the Universal gas constant and $\Delta S_{r,k}$ denotes the reaction entropy of the k th reaction.

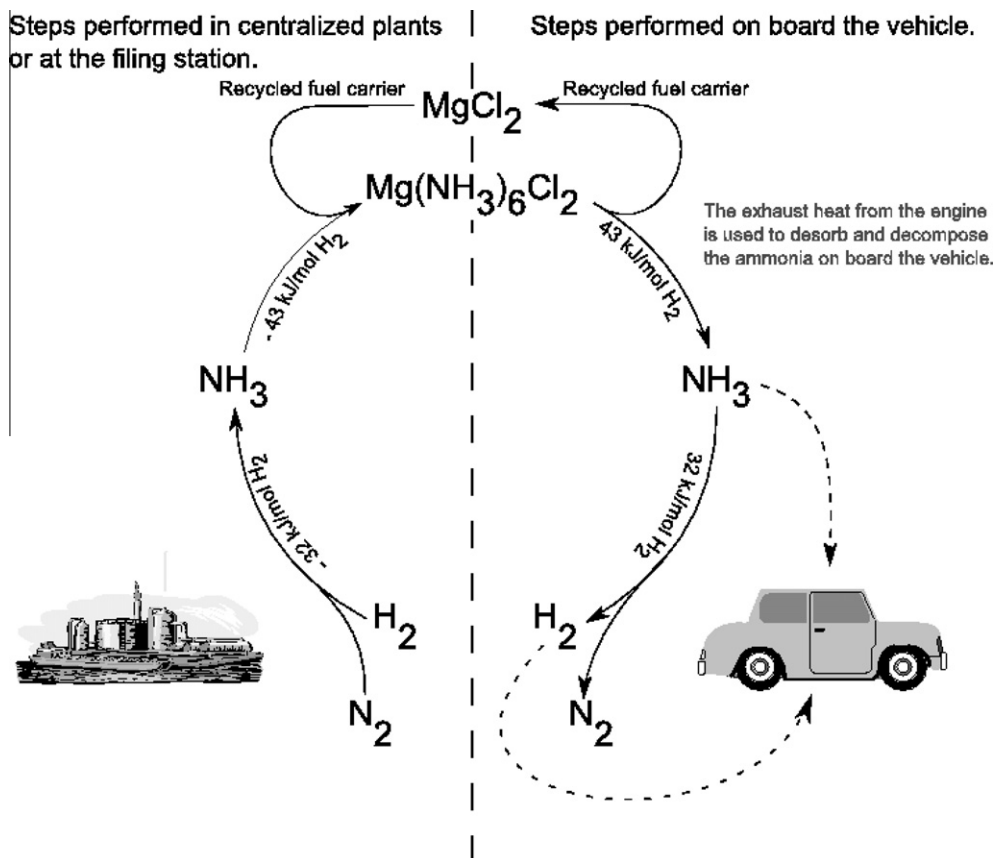


Fig. A1. Using MgCl_2 as hydrogen carrier. The four principle stages of using MgCl_2 as a carrier for hydrogen. In the first stage H_2 and N_2 are (catalytically) synthesized into NH_3 , the next stage consists of the ammonia absorption by MgCl_2 into $\text{Mg(NH}_3)_6\text{Cl}_2$. With the first two steps completed, the ammonia can be transported in a safe manner. When the ammonia or hydrogen is needed, steps 3 and 4 can be completed. Step 3 is the desorption of ammonia from MgCl_2 . The MgCl_2 can be reused to absorb new ammonia. The final step is to (catalytically) decompose ammonia into hydrogen and nitrogen.

A1.2. Energy density

In Fig. A2 a comparison of the energy density of ammonia and hydrogen stored in different forms is made with gasoline. The figure shows that ammonia and hydrogen stored in $\text{Mg(NH}_3)_6\text{Cl}_2$ offer

a feasible storage method regarding the energy density. As Fig. A2 shows, liquid ammonia is actually better than the metal amine approach in energy density matters, but the total fuel system will be heavy and will give a considerable higher safety risk than the metal amine complex in terms of transportation.

A1.3. The proposed fuel system

To evaluate the possibility of using exhaust heat for the fuel system, the principle system set up in Fig. A3 was used. Preliminary calculations showed that the exhaust heat could not cover the full demand of the fuel system. According to Choudhary et al. [21] and Ganley et al. [22] the catalytic decomposition of ammonia requires a temperature of 550–600 °C. This temperature region is higher than the exhaust temperature. In the following analysis the exhaust heat will therefore only be used to desorb the ammonia. It is assumed that the energy for the decomposition and remaining energy for the desorption comes from an external source.

The following assumptions were made in the energy balance calculations on the fuel system.

- Only steady state conditions are considered.
- The exhaust gas is composed of the complete combustion products, obtained for the current operating point by simple stoichiometry.
- Nitrogen from the decomposition of ammonia is not taken into account.
- The complete fuel system including the exhaust pipe is adiabatic.

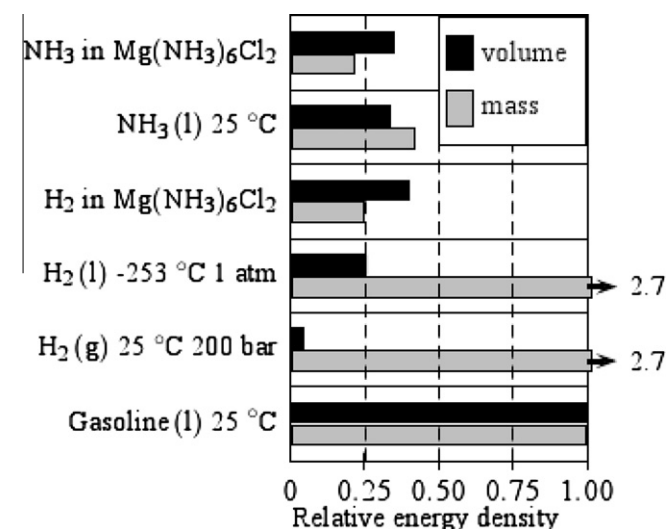
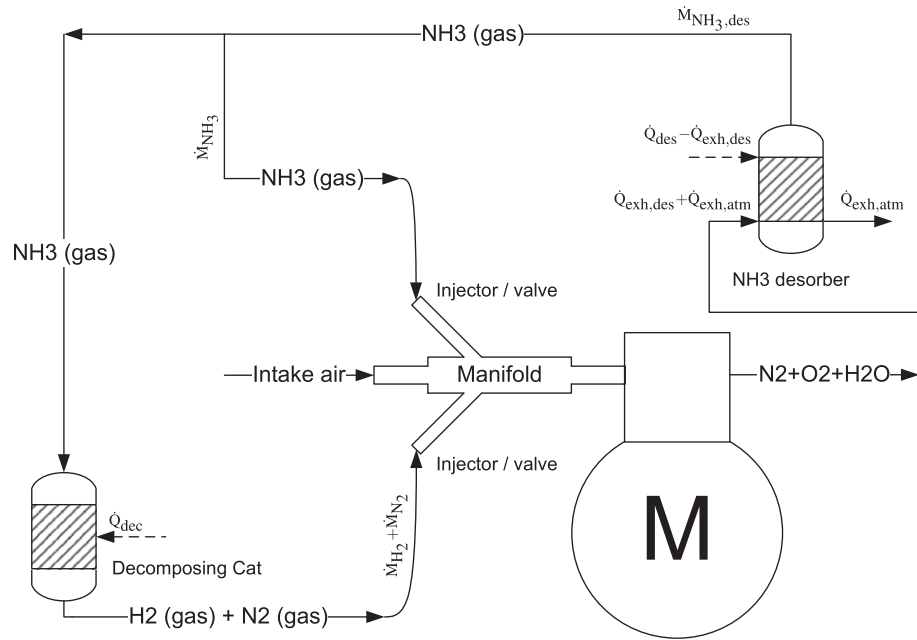


Fig. A2. Energy density. Comparison of the energy density in different hydrogen/ammonia storage methods with gasoline. The densities are normalized so unity represents the value of gasoline. For each alternative the energy density is showed on both mass and volume basis.



- The fuel system is not subject to any pressure losses.
- The desorber temperature is determined by the equilibrium condition defined in Eq. (4).
- The efficiency of the heat exchanger between exhaust gas and desorber is 100%.
- The efficiency of the decomposition catalyst is 100%.

$$\dot{Q}_{exh,des} = \begin{cases} (h_{des,out} - h_{exh}) \cdot \dot{m}_{exh}, & T_{exh} > T_{des} \\ 0, & T_{exh} \leq T_{des} \end{cases} \quad (A8)$$
$$f_{cbe} = \frac{\dot{Q}_{exh,des}}{\dot{Q}_{des} + \dot{Q}_{dec}} \quad (A11)$$

- [1] Verhelst S, Verstraeten S, Sierens R. A comprehensive overview of hydrogen engine design features. *Proc Inst Mech Eng, Part D: J Automob Eng* 2007;221(8):911–20. URL: <http://dx.doi.org/10.1243/09544070JAUTO141>.
- [2] Pearsall J, Garabedian C. Combustion of anhydrous ammonia in diesel engines. *Society of Automotive Engineers – Papers* (670947).
- [3] Sawyer R, Starkman E, Muzio L, Schmidt W. Oxides of nitrogen in combustion products of ammonia fueled reciprocating engine. *Society of Automotive Engineers – Papers* (680401).
- [4] Starkman E, Newhall H, Sutton R, Maguire T, Farbar L. Ammonia as spark ignition engine fuel – theory and application. *Society of Automotive Engineers – Papers* (660155).
- [5] Starkman E, James G, Newhall H. Ammonia as diesel engine fuel – theory and application. *Society of Automotive Engineers – Papers* (670946).
- [6] Gray Jr J, Dimitroff E, Meckel N, Quillian Jr R. Ammonia fuel – engine compatibility and combustion. *Society of Automotive Engineers – Papers* (660156).
- [7] Reiter AJ, Kong S. Demonstration of compression-ignition engine combustion using ammonia in reducing greenhouse gas emissions. *Energy Fuels* 2008;22:2963–71.
- [8] Saika T. Study of an ammonia fueled engine as a clean energy system. *Nihon Enerugi Gakkaishi/Jpn Inst Energy* 2000;79(6):530–9.
- [9] Ferguson CR, Kirkpatrick AT. *Internal combustion engines, applied thermosciences*. second ed. John Wiley & Sons; 2001.
- [10] Hodgson JW. Alternate fuels for transportation – part 3: ammonia for the automobile. *Mech Eng* 1974;96(7):22–5.
- [11] Mørch CS. Performance of ammonia/hydrogen mixtures in si engines. Master's thesis. Department of Mechanical Engineering, Technical University of Denmark, danish language (July 2007).

- [12] Krieger RB, Borman GL. The computation of apparent heat release for internal combustion engines. In: Winter annual meeting and energy systems exposition, New York, NY, November 27–December 1, 1966, No. 66-WA/DGP-4. The American Society of Mechanical Engineers; 1966.
- [13] Eichelberg G. Some new investigations on old combustion engine problems. *Engineering* 148(3850).
- [14] Shudo T, Suzuki H. Applicability of heat transfer equations to hydrogen combustion. *JSAE Rev* 2002;23(3):303–8.
- [15] Taylor C. The internal-combustion engine, vol. second printing. International Textbook Company; 1962.
- [16] Heywood JB. Internal combustion engine fundamentals. McGraw-Hill Book Company; 1988.
- [17] Elmøe T, Sørensen R, Quaade U, Christensen C, Nørskov J, Johannessen T. A high-density ammonia storage/delivery system based on $\text{Mg}(\text{NH}_3)_6\text{Cl}_2$ for SCR-DeNO_x in vehicles. *Chem Eng Sci* 2006;61(8):2618–25.
- [18] Huls T, Myers P, Uyehara O. Spark ignition engine operation and design for minimum exhaust emission. Society of Automotive Engineers – Papers (660405).
- [19] Chorkendorff I, Niemantsverdriet JW. Concepts of modern catalysis and kinetics. Wiley-VCH; 2005.
- [20] Christensen CH, Sørensen RZ, Johannessen T, Quaade UJ, Honkala K, Elmøe TD, et al. Metal ammine complexes for hydrogen storage. *J Mater Chem* 2005;15(38):4106–8.
- [21] Choudhary T, Sivadinarayana C, Goodman D. Catalytic ammonia decomposition: cox-free hydrogen production for fuel cell applications. *Catal Lett* 2001;72(4):197–201.
- [22] Ganley J, Seebauer E, Masel R. Development of a microreactor for the production of hydrogen from ammonia. *J Power Sources* 2004;137(1):53–61.
- [23] Linstrom P, Mallard W, editors. NIST chemistry WebBook, NIST Standard Reference Database Number 69. Gaithersburg MD, 20899: National Institute of Standards and Technology; 2005 (<http://webbook.nist.gov>).

ID	Title	Pages
206680	Ammonia/hydrogen mixtures in an SI-engine: Engine performance and analysis of a proposed fuel system	11

Related Articles



<http://fulltext.study/journal/106>



Categorized Journals

Thousands of scientific journals broken down into different categories to simplify your search



Full-Text Access

The full-text version of all the articles are available for you to purchase at the lowest price



Free Downloadable Articles

In each journal some of the articles are available to download for free



Free PDF Preview

A preview of the first 2 pages of each article is available for you to download for free

<http://FullText.Study>